Determination of Nuclear Reaction Widths from Reaction Yield Curves*

JAMES A. FERRY, G. WENDT,† D. W. PALMER,‡ AND J. M. DONHOWE
University of Wisconsin, Madison, Wisconsin
(Received 2 July 1965)

Problems encountered in measuring narrow resonance widths have been studied utilizing several well-known resonances in the $Al^{27}(p,\gamma)Si^{28}$ reaction. Previous measurements had been limited by imperfections of the gap in the electrostatic analyzer. To correct these defects, the surface of each deflection electrode was lapped to a mirror finish and its surface contour was examined by observing the fringe pattern of an optical interferometric device. Another similar device was used to position and measure the gap of the assembled analyzer. The result is a gap constant to $\pm 0.22\ \mu$ over a 4-mm vertical height for 9/10 of the analyzer length. The proton beam from the analyzer was calibrated for energy spread by using the measured profile of the gap and the resonance of known width near 774 keV. Thick- and thin-target-yield curves taken over the resonances near 992 and 1317 keV were analyzed, using a Monte Carlo technique, which accurately accounts for the proton energy loss. Despite significant improvement in target-chamber vacuum conditions and resolution of the electrostatic analyzer, target and analyzer uncertainties limited the accuracy of the measured widths to $\Gamma = 90 \pm 35$ eV and $\Gamma = 85 \pm 45$ eV for the 992- and 1317-keV resonances, respectively. This study shows that three problems are likely to cause errors in resonance-width and resonance-position measurements. They are: (1) target contamination, (2) treatment of energy loss process, and (3) beam-analyzer imperfections. Examination of methods used previously indicate that these errors tend to compensate. Since compensation under all conditions cannot be expected, this work indicates need for improved measurement methods.

I. INTRODUCTION

THE full width at half-maximum for a narrow isolated $(p\,\gamma)$ resonance can be deduced from the shape of the γ-ray yield as a function of bombarding proton energy if all factors which influence this shape are known. These factors are: (1) the resonance cross section, (2) the Doppler broadening, (3) the incident-energy distribution of protons in the beam, (4) the energy-loss process of the protons in the target, and (5) target imperfections.

In previous measurements of narrow (p,γ) resonance widths, the last three of these factors were treated in the following manner: The beam spread was taken to be that calculated for ideal analyzer geometries; the proton energy loss was treated in the continuous-loss approximation; and the targets were assumed to be composed only of pure aluminum. A series of investigations carried out at Wisconsin by Walters, Palmer, Costello, Skofronick, Morsell and their co-workers,[1–6] and at the Naval Research Laboratory by Bondelid and his co-workers[7] has shown that such treatments were incorrect.

These authors took thick-target yield data over narrow (p,γ) resonances using highly resolved proton beams and found maximum yields at mean beam engies just above the resonance energy. This result, called the Lewis[1,8] effect, proved that the continuous-loss approximation could not be used in treating the proton energy-loss process. New methods which involved Monte-Carlo-type calculations were developed at Wisconsin to carefully follow the details of the proton energy loss in a stopping material. These methods were used to accurately predict the Lewis effect.

Continued study by these authors of resonance yield curves revealed that target imperfections were very important in determining the shape of the observed yield. Sophisticated target-making techniques were found necessary to avoid noticeable contamination effects in thick-target yield data taken using modest beam energy resolutions. Such techniques were not used in previous measurements of narrow (p,γ) resonance widths; therefore contamination must have been present.

One additional effect of interest was found in the experiments done at Wisconsin. The energy resolution of the proton beam was always less than that calculated from the known slit widths of the beam energy analyzer. This discrepancy was due to mechanical imperfections in the analyzer. Because of the similarity of techniques used in constructing energy analyzers, this type of discrepancy may be widespread.

The present experiment was undertaken with the expectation that accurate measurement of very narrow resonances could be realized. However, difficulties were encountered and further developments in methods were required before reliable measurements of resonance widths were achieved. To allow comparison with

* This work was supported in part by the U. S. Atomic Energy Commission.
† Now at Fiskars Electronic Company, Helsinki, Finland.
‡ Now at University of Sao Paulo, Brazil.
[1] W. L. Walters, D. G. Costello, J. G. Skofronick, D. W. Palmer, W. E. Kane, and R. G. Herb, Phys. Rev. Letters **7**, 284 (1961).
[2] W. L. Walters, D. G. Costello, J. G. Skofronick, D. W. Palmer, W. E. Kane, and R. G. Herb, Phys. Rev. **125**, 2012 (1962).
[3] D. W. Palmer, J. G. Skofronick, D. G. Costello, A. L. Morsell, W. E. Kane, and R. G. Herb, Phys. Rev. **130**, 1153 (1963).
[4] D. G. Costello, J. G. Skofronick, A. L. Morsell, D. W. Palmer, and R. G. Herb, Nucl. Phys. **51**, 113 (1964).
[5] J. G. Skofronick, J. A. Ferry, D. W. Palmer, G. Wendt, and R. G. Herb, Phys. Rev. **135**, A1429 (1964).
[6] A. L. Morsell, Phys. Rev. **135**, A1436 (1964).
[7] R. O. Bondelid and J. W. Butler, Phys. Rev. **130**, 1078 (1963).
[8] H. W. Lewis, Phys. Rev. **125**, 937 (1962).

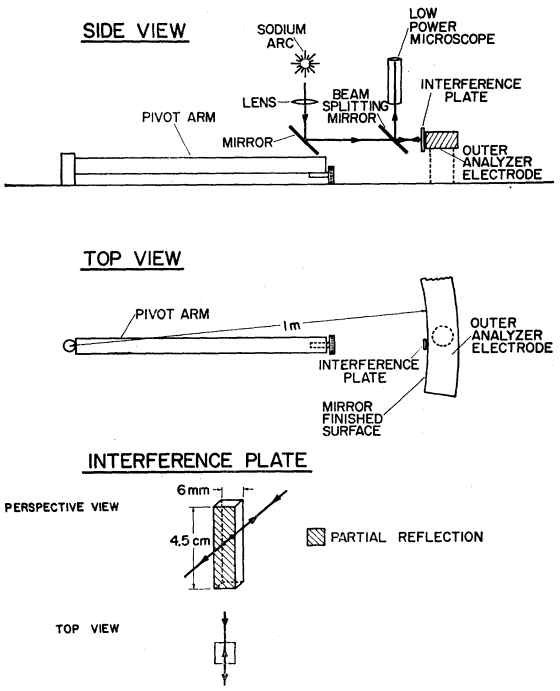

FIG. 1. Schematic diagram of the interferometric device used in finding the surface contour of the outer analyzer electrode.

previous methods, the oft-measured (p,γ) resonances near 992 and 1317 keV in Al^{27} were used.[9–12]

II. EXPERIMENTAL PROCEDURE

A stainless-steel target chamber essentially the same as those described by Costello *et al.*[4] and Skofronick *et al.*[5] was used in this experiment. This chamber was designed to allow many aluminum targets to be prepared and bombarded with no interruption in high vacuum conditions. During the rapid evaporation of a target, the pressure in the chamber was less than 5×10^{-7} Torr and the static pressure during target bombardment was about 1×10^{-8} Torr. These conditions are very similar to those specified by Costello *et al.*[4] and Skofronick *et al.*[5] as adequate for prevention of surface or volume contamination of aluminum targets.

A yield curve was found by the following procedure. A target of the desired thickness was deposited onto a tantalum target backing. The target holder was turned so that the target faced the proton beam which was highly resolved in energy by the use of a one-meter cylindrical electrostatic analyzer. The γ-ray yield from each resonance studied was measured for a particular number of incident protons as a function of the mean beam energy. The γ rays were detected by two NaI(Tl) crystals, one located on each side of the target holder. Each crystal was coupled to a photomultiplier tube which in turn was connected to an amplifier, discriminator, and scalar circuit. The proton current was measured by the use of a current integrator and the mean beam energy was selected for each datum point by changing the potential difference across the electrodes of the electrostatic analyzer.

A. The Electrostatic Analyzer

Before amassing γ-ray yield data on which the desired width measurements could be based, a careful reworking of the electrostatic analyzer was undertaken.[13] The motives behind the reworking and some of the techniques involved will be discussed.

Analysis shows that ideally the proton intensity distribution emerging from a symmetric electrostatic analyzer, as a function of proton energy, will be an isosceles triangle centered at the mean beam energy E_B. The resolution R is defined as $R=E_B/\Delta E_B$, where ΔE_B is the full width at half-maximum of the triangle. In this case R is easily predicted from the analyzer geometry.

In practice the predicted resolution may not be attained because the actual analyzer deviates considerably from the ideal. This had become increasingly evident during studies relating to the Lewis effect done at Wisconsin where resolutions greater than $R=1000$ were desired.[1–6] Morsell[14] and Skofronick[15] had found the primary reason for the discrepancy between a predicted resolution of $R=10\,000$ and the actual resolution attained, to be that the gap between the deflecting electrodes in the analyzer had a wedge-shaped vertical profile.

The general rule which an analyzer gap must satisfy was stated by Warren[16] and is that any systematic fractional variation of the gap width $\Delta d/d$ in the vertical region of the gap through which the beam passes must be small when compared to the desired fractional variation of the beam energy $\Delta E/E$. The analyzer used by Skofronick[15] was found to have a value for $\Delta d/d$ which limited the resolution to about $R=4000$ even when the vertical height of the incident beam was reduced to 1 mm. For this reason a program was undertaken to improve the analyzer gap.

The deflection electrodes were removed from the analyzer vacuum box and were mounted in a convenient

[9] R. S. Bender, F. C. Shoemaker, S. G. Kaufmann, and G. M. B. Bouricius, Phys. Rev. **76**, 273 (1949).

[10] R. O. Bondelid and C. A. Kennedy, Phys. Rev. **115**, 1601 (1959).

[11] A. Rytz, H. H. Staub, H. Winkler, and W. Zych, Helv. Phys. Acta **35**, 341 (1962).

[12] S. L. Anderson, H. Bö, T. Holtebekk, O. Lönsjö, and R. Tangen, Nucl. Phys. **9**, 509 (1959).

[13] J. A. Ferry, Ph.D. thesis, University of Wisconsin, 1965 (unpublished); available from Ann Arbor Microfilms, Inc., Ann Arbor, Michigan.

[14] A. L. Morsell, Ph.D. thesis, University of Wisconsin, 1963 (unpublished); available from Ann Arbor Microfilms, Inc., Ann Arbor, Michigan.

[15] J. G. Skofronick, Ph.D. thesis, University of Wisconsin, 1964 (unpublished); available from Ann Arbor Microfilms, Inc., Ann Arbor, Michigan.

[16] R. E. Warren, Ph.D. thesis, University of Wisconsin, 1947 (unpublished).

position on a surface plate. The electrode surfaces which faced the gap were honed and lapped by simple hand methods until approximately true and were then polished to a mirror finish. The precise surface contour of each electrode was measured with an interferometric device. A schematic diagram of the apparatus used with the outer electrode is shown in Fig. 1. The sodium arc, lens, mirror, beam-splitting mirror, and interference plate were held from the pivot arm and could be moved to any angular position along the analyzer electrode. Fringe patterns which arose from interference between light reflected from the partially reflecting surface of the interference plate and the mirror finished surface of the electrode were viewed through a low-power microscope at many angular positions along the electrode.

Figure 2 shows simplified drawings of a typical sequence of fringe patterns which were observed at 1-cm intervals along each electrode. The fringes are of the type commonly called fringes of equal thickness.[17] Any one fringe designates a line where the distance between the interference plate and the electrode surface is constant; while the position of adjacent fringes shows where this distance has changed by one-half wavelength of sodium light. Analysis of fringes taken along both electrodes showed that a 6-mm region centered about 3 mm below the mid-line was relatively uniform.

The electrodes were then remounted in the analyzer vacuum box on three supports. These supports allowed

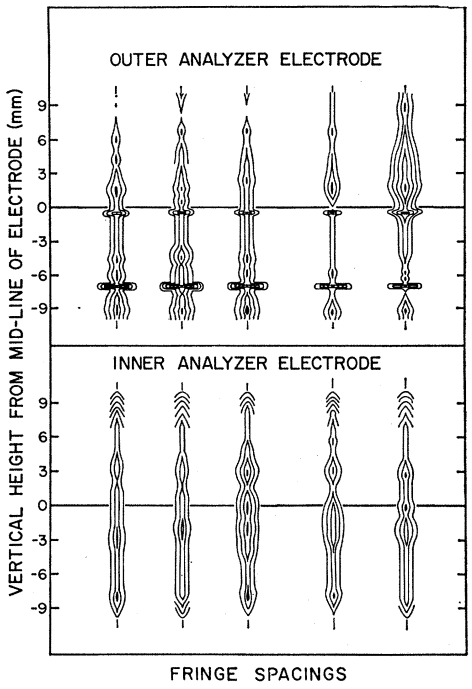

FIG. 2. Simplified drawings of typical sequences of fringe patterns observed at 1-cm intervals along each electrode.

[17] F. A. Jenkins and H. E. White, *Fundamentals of Optics* (McGraw-Hill Book Company, Inc., New York, 1957), Chap. 14.

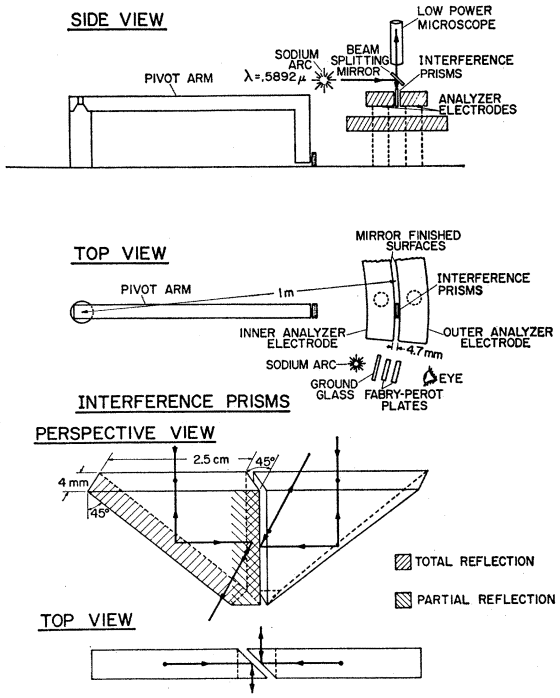

FIG. 3. Schematic diagram of the interferometric device used in finding the profile of the analyzer gap.

modest twisting stresses to be applied to the electrodes and in addition they mechanically decoupled the vacuum box from both the electrodes and the surface plate on which the analyzer rested. Therefore, the electrodes which could be stressed slightly during alignment would not be disturbed when the vacuum box was bolted together and evacuated.

The analyzer electrodes were accurately positioned using a special interferometric device which is shown schematically in Fig. 3. This device employed the same type of interference that was used in finding the surface contours of the electrodes. The interference plate and mirror were replaced by two prisms, one for each electrode. Fringe patterns arose from the interference of reflections off the prisms and the analyzer electrodes.

In measuring the profile of the gap, the partially reflecting surfaces of the prisms were required to be accurately parallel. This was accomplished by swinging the prisms into the accurate gap between a pair of plates from a Fabry-Perot etalon and then adjusting each prism to be parallel with the Fabry-Perot plate it faced.

The profile of the analyzer was precisely measured by swinging the accurately aligned prisms into the gap and observing the fringe patterns at many positions along the arc of the electrodes. By slight twisting of the electrodes by clamps at the support positions, the final gap was aligned to have variation of no more than 0.44μ over a 4-mm vertical height for 90% of the analyzer length.

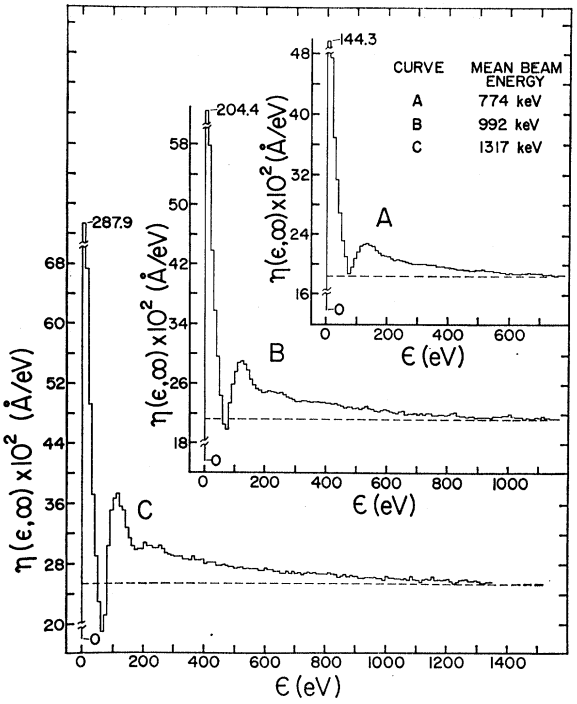

FIG. 4. Energy distribution functions $\eta(\epsilon,\infty)$ in a thick aluminum target. The solid-line histograms are the results of Monte Carlo calculations that accurately account for the proton energy loss. The dashed lines are inverses of the stopping power at each mean proton energy (continuous-loss approximation).

The criteria given earlier allowed an upper limit to the resolution of the corrected analyzer to be established. This could be done since the profile of the analyzer gap had been measured and the vertical height of the proton beam was known to be 3.2 mm at the object slits and 1.5 mm at the image slits. When the object and image slits were set to give theoretical resolutions of either 5000 or 10 000, the actual resolutions of the analyzer were limited to less than 4750 and 8000, respectively.

The maximum values of resolution could have been increased by putting an auxiliary vertical stop near the entrance to the analyzer. This was not tried for two reasons. First, without auxiliary limiting, the beam current near 992 and 1317 keV was only about 40 nA when the theoretical resolution $R_C=5000$ and 20 nA when $R_C=10\,000$. These currents were about double that which could be achieved with the same resolutions when the mean beam energy was near 774 keV. Second, prior to extensive analysis of the experimental data, the actual resolution was thought to be closer to the ideal.

Minimum values of the attained resolution could not be estimated from analyzer geometry alone. Therefore, an experimental technique described in Sec. IV was used to find them.

III. COMPUTATIONAL PROCEDURE

The γ-ray yield from an isolated resonance at energy E_R for N protons with mean beam energy E_B incident on a target of thickness t can be written as

$$Y(E_B,t)=N\int_0^\infty dE\,\sigma(E)\int_0^\infty dE_i\,g(E_B,E_i)\int_0^t dx \times n(x)W(E_i,E,x), \quad (1)$$

where $\sigma(E)$ is a Breit-Wigner cross section modified to include the Doppler broadening; $g(E_B,E_i)$ is the normalized distribution in energy of particles in the incident beam which has a mean energy E_B; $W(E_i,E,x)dE$ is the probability that a particle incident at energy E_i will have an energy between E and $E+dE$ at a distance x in the target; and $n(x)$ is the number of disintegrable nuclei per cm³. Equation (1) can be simplified by making several approximations.

The functions $W(E_i,E,x)$ and $g(E_B,E_i)$ can be assumed to depend only on E_i-E and E_B-E_i, respectively, over the relatively small energy interval about each resonance studied. The targets are assumed to be uniform and noncontaminated so that $n(x)=n$, where n is a constant. Errors introduced by this approximation are discussed in Sec. VI. The modified cross section $\sigma(E)$ can be separated into a Breit-Wigner shaped function which accounts for the reaction cross section and a Gaussian-shaped function which accounts for the Doppler broadening. This form of the cross section had been derived for a crystalline solid by Lamb.[18]

Using these assumptions and making the substitutions $\epsilon=E_i-E$ and $\eta(\epsilon,t)=\int_0^t dx W(\epsilon,x)$, Eq. (1) can be written as

$$Y(E_B,t)=\text{const}N\int_0^\infty d\epsilon\,\eta(\epsilon,t)\int_{-\infty}^\infty dE_1\,\sigma_\Gamma(E_1-E_R)\int_0^\infty dE \times g[(E_B-\epsilon)-E]\sigma_\Delta(E-E_1), \quad (2)$$

where the function

$$\sigma_\Gamma(E_1-E_R)=[1+(E_1-E_R)^2(4/\Gamma^2)]^{-1}$$

has the Breit-Wigner shape and a full width at half-maximum Γ; and the function

$$\sigma_\Delta(E-E_1)=\exp[-5.54(E-E_1)^2/2\Delta^2]$$

has the Gaussian shape and a full width at half-maximum $\Delta=107\,(E_B \text{ in MeV})^{1/2}$ eV.

The form of the two functions $\eta(\epsilon,t)$ and $g[(E_B-\epsilon)-E]$ remains to be specified before yield curves can be calculated from Eq. (2). The beam spreading function $g[(E_B-\epsilon)-E]$ was assumed to have the shape calculated for an ideal cylindrical analyzer, i.e., to be an isosceles triangle centered at the mean beam energy. The full width at half-maximum of the triangle was assumed to be $\Delta E_B=E_B/R$ where R is the actual resolution of the analyzer.

The energy distribution function $\eta(\epsilon,t)$ has a very simple form for a target of vanishing thickness, $\eta(\epsilon,0)$

[18] W. E. Lamb, Jr., Phys. Rev. 55, 190 (1939).

$\propto \delta(\epsilon)$.[3] For targets of finite thickness no simple functional form can be found. In this paper, the form of $\eta(\epsilon,t)$ will be considered for the particular case of a target of infinite thickness, i.e., a target of a sufficient thickness so that a plateau yield can be defined.

A Monte Carlo method was used for finding $\eta(\epsilon,\infty)$. The techniques used in the Monte Carlo calculation of $\eta(\epsilon,\infty)$ were essentially identical to those described by Walters *et al.*[2] and Costello *et al.*[4] In the present calculation, the cross section for a discrete energy loss as a function of the value of the energy loss was of the type used by Skofronick *et al.*[5] In addition, better statistical accuracy of $\eta(\epsilon,\infty)$ was demanded here than in previous calculations.[13] Figure 4 shows the $\eta(\epsilon,\infty)$ functions used in this work.

IV. RESULTS

1. *The resonance at 774 keV.* Yield curves taken over the $Al^{27}(p,\gamma)Si^{28}$ reaction near 774 keV were studied for the purpose of determining a minimum value for the actual resolution of the electrostatic analyzer. This was possible because the width of the resonance near 774 keV had been previously measured. Smith and Endt[19] found the value $\Gamma=9.0\pm0.8$ eV employing the resonant absorption in silicon of the γ rays produced by the reaction. Their work has been re-analyzed by Endt[20] using recent unpublished absolute yield measurements of Nordhagen and Smith with the new result $\Gamma=14\pm3$ eV. The method used in the measurement of this width should not be susceptible to errors of the type mentioned in the Introduction.

Figure 5 shows experimental data taken, using aluminum targets of average thickness 9, 10, and 11Å in parts A, B, and C, respectively. For this data the analyzer slits were set to give a theoretical resolution of 5000. The curves superposed on the data were calculated[21] using Eq. (2), where $\Gamma=14$ eV, $\Delta=94$ eV, and $\Delta E_B=130$, 190, or 250 eV. In all the calculated curves the function $\eta(\epsilon,0)$ was taken to be $\delta(\epsilon)$.

Figures 6 and 7 show experimental thick-target γ-ray yield data taken with the electrostatic analyzer slits set to give ideal resolutions of $R_C=5000$ and $R_C=10\,000$, respectively. The theoretical curves superposed on the experimental points were calculated by numerical integration of Eq. (2). The functions in this equation were constructed using the widths $\Gamma=14$ eV, $\Delta=94$ eV, and $\Delta E_B=130$, 190, or 250 eV in Fig. 6 and $\Delta E_B=70$, 130, or 190 eV in Fig. 7. The function $\eta(\epsilon,\infty)$ was that determined by the Monte Carlo method.

The uncertainty in relative yield for all experimental

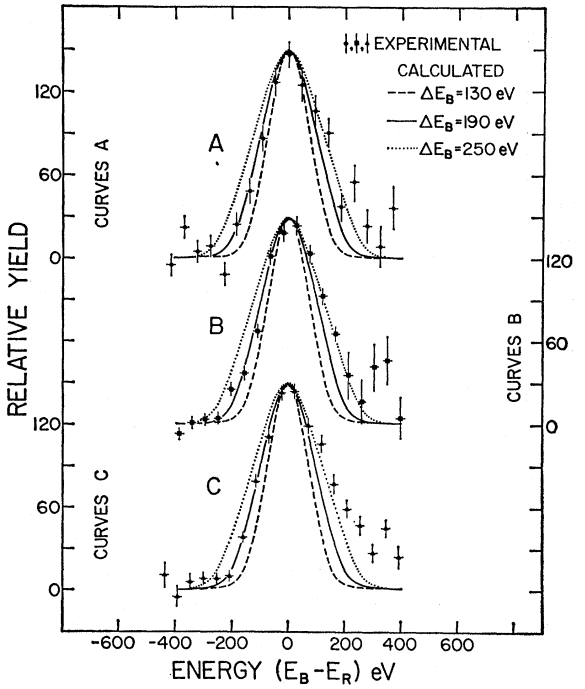

FIG. 5. Experimental thin-target yield data taken over the $Al^{27}(p,\gamma)Si^{28}$ resonance near 774 keV with the analyzer slits set for an ideal beam width $\Delta E_B=155$ eV. The curves shown are calculated for three values of ΔE_B.

data has been assigned on a statistical basis. For data taken using very thin targets, uncertainty in relative energy E_B-E_R also had to be assigned. Early in the present experiment the energy analyzer was found to allow the mean beam energy to drift in one direction throughout a day of data taking at a rate of about 0.002 percent per hour. This small drift could affect thick-target yield data only at the few points where the yield is increasing rapidly with beam energy. Uncertainty in these points could be kept small by taking them in quick succession. However, running times of about 2 h were necessary when using very thin targets to achieve reasonable statistical accuracy in the relative yield. Since almost every point in a thin-target yield curve is affected by beam-energy drift, an uncertainty in relative energy had to be assigned.

The experimental data and theoretical curves of Figs. 5 through 7 show a consistent pattern of disagreement. The thin-target yield points for positive relative energy are higher than the theoretical curves and the thick-target yield points in the energy region of their peak values are lower than the theoretical curves. This behavior can be explained if the thin targets were not of uniform thickness and if the thick and thin targets were contaminated.[3,5,7]

Prior to extensive analysis it was thought that target contamination was not significantly affecting the yield curves found in the present experiment. Target conditions had been maintained close to the values suggested

[19] P. B. Smith and P. M. Endt, Phys. Rev. **110**, 397 (1958).
[20] P. M. Endt (private communication).
[21] The calculated curves shown throughout this paper have been chosen to demonstrate how the shape varies with resolution or resonance width. Many additional theoretical curves were calculated which fit the experimental data closely. However, such curves are difficult to display clearly and are not shown in this paper.

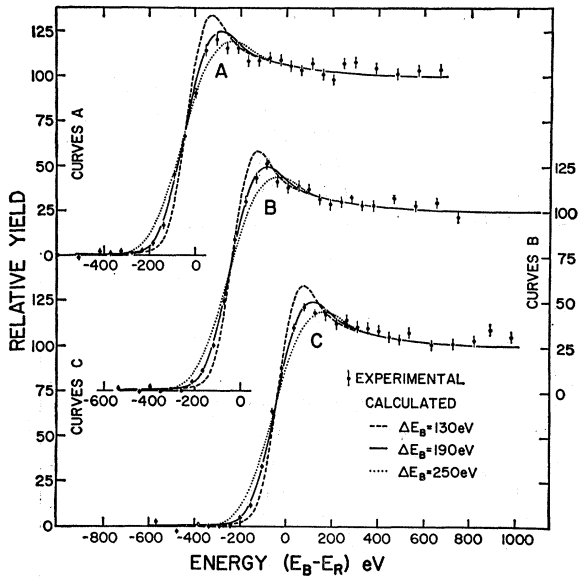

FIG. 6. Experimental thick-target yield data taken over the $Al^{27}(p,\gamma)Si^{28}$ resonance near 774 keV with the analyzer slits set for an ideal beam width $\Delta E_B=155$ eV. The curves shown are calculated for three values of ΔE_B. During the actual analysis of the data many intermediate values of ΔE_B were used in theoretical curves.

by Costello *et al.*[4] The failure of these conditions in preventing contamination effects was probably due to the increase in beam resolution from about 3000 used by Costello *et al.*[4] to the higher values used in this experiment.

Palmer *et al.*[3] have shown qualitatively that target imperfections of the types mentioned above always cause a decrease in the slope of a resonance yield curve with respect to that from a perfect target in the energy region below the resonance energy. Therefore, an upper limit to the combined total of the beam, Doppler, and resonance widths can be established even though the precise effect of target imperfections is unknown. The height of the Lewis peak is particularly sensitive to target imperfections and could not be used in these measurements to determine the spreading factors.

In the specific case of the 774-keV resonance, the Doppler broadening and resonance width are known[22]; therefore a limit can be placed on the analyzer resolution by finding the beam width which gives the best theoretical fit to the experimental data in the energy regions of the plateau yield and below the resonance energy. Analysis of the thick-target data taken over this resonance showed that when the analyzer slits were set to give a theoretical resolution R_C of 5000 and 10 100 the actual resolution R obtained could not be less than 4030 and 6000, respectively. The large experimental uncertainty did not allow accurate limits to be determined using the thin-target data. However, results obtained from the thick-target analysis give reasonable fits to the thin-target data.

The lower limits found using the 774-keV resonance can be combined with the upper limits found using the gap measurements to give the actual resolution of the analyzer. Thus when the theoretical resolution R_C is 5000, the actual resolution is between 4030 and 4750, and when R_C is 10 100, R is between 6000 and 8000.

2. *The resonances at 992 and 1317 keV.* Yield curves taken over the $Al^{27}(p,\gamma)Si^{28}$ resonances near 992 and 1317 keV were studied to determine the full widths at half-maximum Γ of these resonances. Such a determination was made possible by using the values for the resolution of the electrostatic analyzer found previously.

Figure 8(A) and 8(B) show experimental γ-ray yield data taken over the 992-keV resonance from targets of 10.5 and 4 Å average thickness, respectively, when the theoretical resolution R_C of the incident proton beam was 5000. Figure 8(C) shows the yield from a target of average thickness of 5 Å when $R_C=10\,100$. The curves superposed on the experimental points were calculated by numerical integration of Eq. (2). In this calculation the values used for the Breit-Wigner width Γ were 40 eV in the dashed curve, 90 eV in the solid curve, and 140 eV in the dotted curve. In all curves the Doppler width Δ was taken to be 107 eV, and the energy distribution function $\eta(\epsilon,0)$ to be $\delta(\epsilon)$. The curves in parts A and B were calculated using a beam width $\Delta E_B=228$ eV, while for those in part C, $\Delta E_B=144$ eV.

Figure 9, parts A, B, and C show experimental-yield data taken over the 992-keV resonance using thick targets and theoretical resolution of the analyzer $R_C=5000$ in parts A and B, and $R_C=10\,100$ in part B.

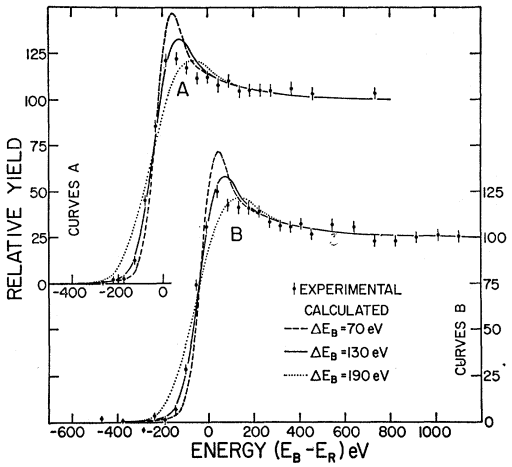

FIG. 7. Experimental thick-target yield data taken over the $Al^{27}(p,\gamma)Si^{28}$ resonance near 774 keV with the analyzer slits set for an ideal beam width $\Delta E_B=77$ eV. The curves shown are calculated for $\Delta E_A=70$, 130, and 190 eV. During the actual analysis of the data many more values of ΔE_B were used.

[22] Throughout this work it has been assumed that uncertainties in the Doppler-broadening function σ_Δ, the energy-distribution function η, and the shape of the beam-spreading function g are negligible in comparison to uncertainties introduced by target and analyzer imperfections. Qualitative studies and related work indicate that these assumptions are justified.

The curves superposed on the experimental data were calculated by numerical integration of Eq. (2). In the calculated curves, the Breit-Wigner width Γ was set equal to 40 eV in the dashed curve, 90 eV in the solid curve, and 140 eV in the dotted curve; the Doppler width Δ was set equal to 107 eV; and the function $\eta(\epsilon,\infty)$ was that determined by the Monte Carlo calculation. The beam width ΔE_B was set equal to 228 eV in parts A and B, and 144 eV in part C.

Figure 10 shows two sets of experimental yield data taken over the 1317-keV resonance using thick targets and theoretical resolution $R_C=10\,100$. The curves superposed on the experimental points were calculated from Eq. (2) using a numerical-integration procedure. In this equation, the Breit-Wigner width Γ was assumed to have one of three values, 25, 85, or 145 eV; the Doppler width Δ was taken to be 122 eV; and the beam width ΔE_B was set equal to 191 eV. The energy distribution function $\eta(\epsilon,\infty)$ was that determined by the Monte Carlo calculation.

Experimental uncertainty for data taken over the resonances near 992 and 1317 keV has been assigned in a manner completely analogous with that used for data taken over the resonance near 774 keV and described in the preceding section.

As in the 774-keV data, target imperfections are evident in the yield data taken over the 992- and 1317-keV resonances. For this reason analysis of the type used to determine the actual resolution must be used to find the resonance width. An upper limit to the resonance width was determined by finding the maximum Γ which allowed the experimental yield data to be fitted in the energy region of increasing yield with theoretical curves calculated using the minimum value of ΔE_B. A lower limit of Γ was much more difficult to find. A qualitatively correct computation was made using the 774-keV data which estimated the maximum target contamination required to reduce the peak yield of a theoretical thick-target curve to experimentally

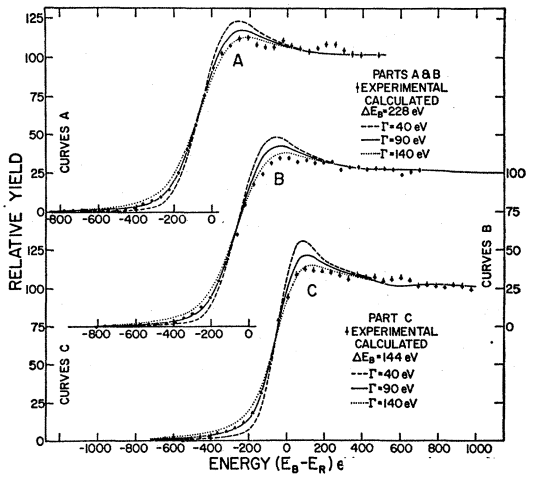

FIG. 9. Experimental thick-target yield data taken over the $Al^{27}(p,\gamma)Si^{28}$ resonance near 992 keV with the analyzer slits set for an ideal beam width of 198 eV in parts A and B and 98 eV in part C. The curves are calculated using the beam widths ΔE_B $=228$ eV in parts A and B, and $\Delta E_B=144$ eV in part C and the resonance widths Γ shown. In the determination of the resonance width, a much larger variety of curves were tried than shown here.

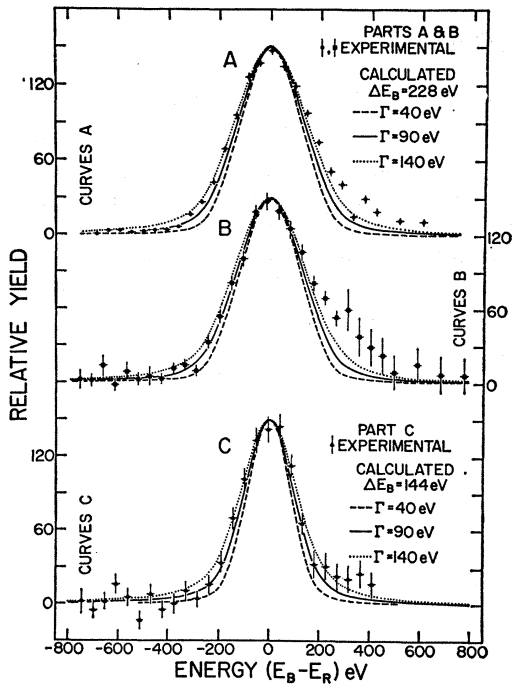

FIG. 8. Experimental thin-target yield data taken over the $Al^{27}(p,\gamma)Si^{28}$ resonance near 992 keV with the analyzer slits set for an ideal beam width of 198 eV in parts A and B and 98 eV in part C. The curves are calculated using the beam widths ΔE_B $=228$ eV in parts A and B, and $\Delta E_B=144$ eV in part C and the resonance widths Γ shown.

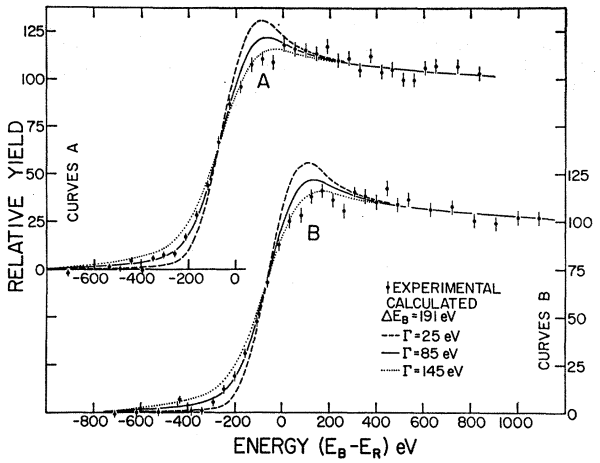

FIG. 10. Experimental thick-target yield data taken over the $Al^{27}(p,\gamma)Si^{28}$ resonance near 1317 keV with the analyzer slits set for an ideal beam width of 130 eV. The curves are calculated using the beam width $\Delta E_B=191$ eV and the values of Γ shown. In the determination of the resonance width, a much larger variety of curves were tried than shown here.

observed values. In this case the theoretical curve was calculated using the minimum value of ΔE_B so that contamination effects were maximized. Then assuming this estimate of target contamination to be correct for the 992- and 1317-keV data, a computation was made to find the minimum value of Γ which allowed the experimental data to be fitted with theoretical thick-target curves calculated using the maximum value of ΔE_B.

The resonance width was assigned as the mean of the upper and lower limits of Γ with uncertainties determined by these limits. The data taken near 992 and 1317 keV indicated resonances with widths $\Gamma=90\pm35$ eV and $\Gamma=85\pm45$ eV, respectively.[23]

V. CONCLUSIONS

The primary objective of this experiment was a highly accurate measurement of the width of a few resonances. This objective was not achieved. Progress, however, was made toward a clear understanding of the problems to be met. Extensive analysis of the data showed the major causes of difficulty to be target contamination and beam-analyzer imperfections.

A review of target conditions may help put the contamination problem in its proper perspective. The target chamber was of stainless-steel construction with all parts sealed by means of aluminum gaskets. A static pressure of 1×10^{-8} Torr or less was normally maintained in the chamber. This was achieved by initially baking the chamber for about 20 h near 300°C at mechanical forepump pressure. Then upon cooling the target chamber pressure was quickly reduced to static conditions by a titanium getter-ion pump contained in the chamber. Targets were deposited by evaporation of ultrapure aluminum wire in the evacuated chamber in total elapsed times of 40 sec or less during which time the target chamber pressure rose to 5×10^{-7} Torr or less. Subsequent use of such targets starting approximately 10 min after deposition and sometimes extending over a period of several days never showed any significant change in yield curve shape. This was interpreted prior to data analysis as demonstrating that target contamination was not occurring. In retrospect, the existence of target contamination is not surprising. A simple calculation of the number of atoms impinging on a clean surface in a vacuum of 1×10^{-7} Torr shows that about 20 sec are required for the formation of a monoatomic layer of contaminant. Therefore in a critical period during or immediately following deposition of a clean aluminum target several monolayers of a comparatively inert surface contaminant could have formed. Such contamination can easily cause the effects found in this work.

The contribution of this experiment can be summarized as showing that present techniques are not good enough for an accurate determination of a narrow resonance width from a resonance yield curve. Work is under way at Wisconsin to reduce the target chamber pressure to the 10^{-10}-Torr region where surfaces can be expected to remain atomically clean for several hours. In addition the intensity of the proton beam is being improved. This will allow some vertical stopping of the beam passing through the electrostatic analyzer and may improve resolution. Preliminary results indicate that these improvements will be at least partially successful.

[23] Additional analysis has shown that the values reported by the present authors at the 1964 autumn meeting of the American Physical Society at Chicago were optimistic and that the present values are more realistic.

ACKNOWLEDGMENTS

The authors are grateful to Professor R. G. Herb for his active support and guidance during the course of this work. The helpful discussions and assistance of Professor E. E. Miller with regard to the interferometric devices are appreciated. The authors also wish to thank W. G. Mourad, R. J. Nickles, and K. E. Nielsen for their valuable aid.